X-ray scattering measurements on imploding CH spheres at the National Ignition Facility

D. Kraus,[1,*] D. A. Chapman,[2,3] A. L. Kritcher,[4] R. A. Baggott,[2] B. Bachmann,[4] G. W. Collins,[4] S. H. Glenzer,[5]
J. A. Hawreliak,[4,6] D. H. Kalantar,[4] O. L. Landen,[4] T. Ma,[4] S. Le Pape,[4] J. Nilsen,[4] D. C. Swift,[4] P. Neumayer,[7]
R. W. Falcone,[1] D. O. Gericke,[2] and T. Döppner[4,†]

[1]*Department of Physics, University of California, Berkeley, California 94720, USA*
[2]*Centre for Fusion, Space and Astrophysics, Department of Physics, University of Warwick, Coventry CV4 7AL, United Kingdom*
[3]*Plasma Physics Group, Radiation Physics Department, AWE plc, Reading RG7 4PR, United Kingdom*
[4]*Lawrence Livermore National Laboratory, Livermore, California 94550, USA*
[5]*SLAC National Accelerator Laboratory, Menlo Park, California 94309, USA*
[6]*Institute for Shock Physics, Washington State University, Pullman, Washington 99164, USA*
[7]*GSI Helmholtzzentrum für Schwerionenforschung, 64291 Darmstadt, Germany*

We have performed spectrally resolved x-ray scattering measurements on highly compressed polystyrene at pressures of several tens of TPa (100 Mbar) created by spherically convergent shocks at the National Ignition Facility. Scattering data of line radiation at 9.0 keV were recorded from the dense plasma shortly after shock coalescence. Accounting for spatial gradients, opacity effects, and source broadening, we demonstrate the sensitivity of the elastic scattering component to carbon K-shell ionization while at the same time constraining the temperature of the dense plasma. For six times compressed polystyrene, we find an average temperature of 86 eV and carbon ionization state of 4.9, indicating that widely used ionization models need revision in order to be suitable for the extreme states of matter tested in our experiment.

Matter under extreme pressures, otherwise only occurring in astrophysical objects [1], can nowadays be created in the laboratory applying laser-driven implosions at the National Ignition Facility. Mostly, such experiments aim for inertial confinement fusion [2,3] where the ablator material reaches pressures exceeding 10 TPa (100 Mbar) and temperatures on the order of 10^6 K (100 eV). Precise knowledge of the material properties under these conditions is crucial for the design of efficient implosions as well as modeling the state and evolution of planets and dwarf stars.

The ionization balance plays a crucial role when modeling states under large pressures. In particular, the level of K-shell ionization for carbon or beryllium is predicted to strongly influence the shock Hugoniot at pressures between 10 TPa and 1 PPa [4] and, thus, the hydrodynamic response in inertial fusion experiments. Models describing the ionization balance in hot, dense matter can be roughly divided into two classes: the first one includes shell effects, i.e., the discrete bound state energies of ions, whereas orbital-free descriptions, like the frequently used Thomas-Fermi model, yield a continuous spectrum of states. For heavier elements or extremely high densities, the latter approach is often a well-justified simplification. However, recent experiments showed significant deviations for light elements in the warm dense matter regime where Thomas-Fermi models underestimate ionization [5,6]. Moreover, the extended distributions of ionization levels predicted for high temperatures cannot be reproduced by average atom models.

In dense matter, the bound states, and accordingly the ionization balance, are modified by the interaction with the surrounding medium. In particular, the influence of neighboring ions and screening due to continuum electrons results in reduced binding strength, which can be modeled by introducing effective (lower) ionization energies. Although a precise description of the complex interaction of a dense plasma with bound states is still incomplete, the Stewart and Pyatt model [7], interpolating between known limits, is thought to catch the essential physics and is widely applied. Experiments creating hot, solid-density aluminum by isochoric heating with x rays have recently challenged this view, indicating a significantly larger depression of the ionization energy [8,9], whereas other experiments are in line with this description [10].

With our present results, we vastly extend the range of states investigated by employing convergent shocks driven by 176 laser beams at the National Ignition Facility. Creating pressures exceeding 10 TPa, electron densities of more than 10^{24} cm^{-3} and temperatures of 100 eV are reached in a solid polystyrene sphere. These conditions result in predicted ionization potential depressions of more than 100 eV for C^{4+} ions, approaching the K-shell ionization energy. The sample is tested by x-ray Thomson scattering (XRTS) [11] using x rays from a laser-produced Zn source. The spectrum obtained contains information on the basic plasma properties and is particularly sensitive to inner-shell ionization. Detailed modeling and analysis of our experimental results support a significantly higher carbon ionization state than predicted by both the Thomas-Fermi model post-processing the hydrodynamic simulations as well as the widely used Stewart and Pyatt approach.

The experiment was performed within the Gbar equation of state (EOS) campaign [12] of the fundamental science program at the National Ignition Facility (NIF). A schematic of the experimental setup is shown in Fig. 1. Here, a standard inertial confinement fusion (ICF) gold hohlraum with near-vacuum gas fill [13] is irradiated by 176 laser beams delivering a

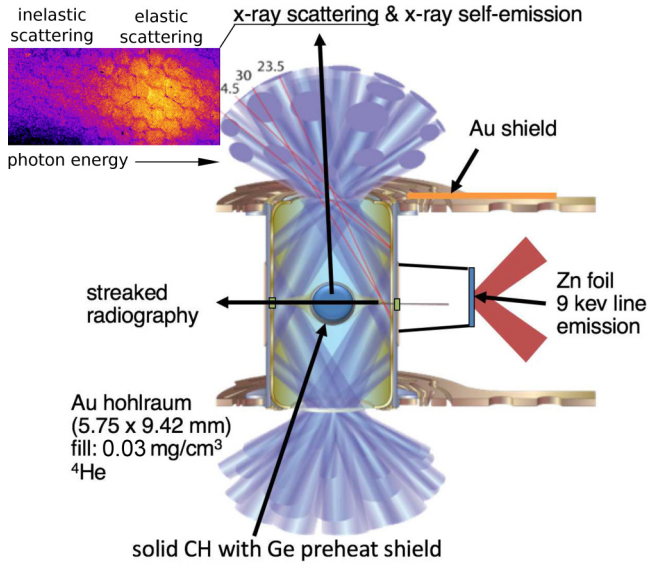*d.kraus@hzdr.de
†doeppner1@llnl.gov

FIG. 1. Experimental setup of the Gbar EOS fundamental science experiments.

total energy of 1.1 MJ and a peak power of 425 TW. The resulting radiation field drives a spherical implosion of a solid polystyrene (CH) sphere with 1.15 mm radius positioned in the center of the hohlraum. Radial profiles of density and temperature were obtained by hydrodynamics simulations using HYDRA [14] with the LEOS 5350 equation-of-state table for polystyrene. The density profile and the temperature of the hot plasma in the center are in good agreement with simultaneous radiography and hot spot measurements [15,16]. Ionization was calculated by the Thomas-Fermi model post-processing the HYDRA calculations (Fig. 2). The simulations show that the shock drive produces a plasma with significant radial gradients resulting in three distinct regions: a hot, highly compressed core, a large region of dense material moving inward towards the core, and a hot corona of ablated material.
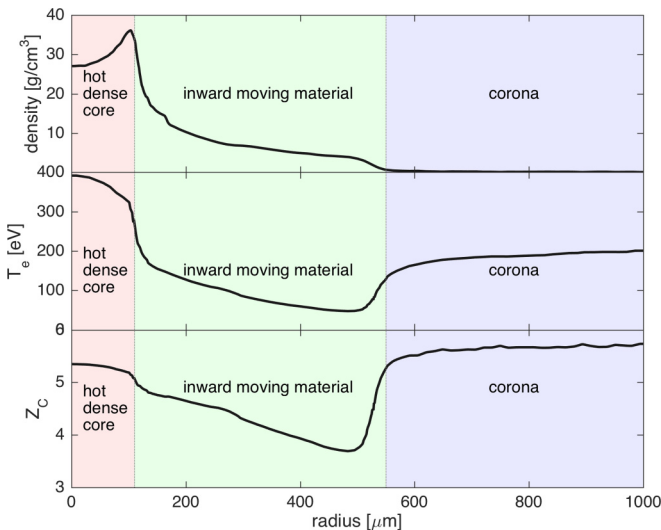

FIG. 2. Post-experiment simulations of the radial profiles of the basic plasma parameters as obtained from the radiation-hydrodynamics code HYDRA 480 ps after shock stagnation.

The high-energy radiation used to probe the sample is created by another 16 laser beams focused onto a 15-μm-thick zinc foil that is mounted at 7.5 mm distance from the center of the CH sphere. The hot zinc plasma produces intense line emission of helium-like ions (Zn He-α) at 9.0 keV photon energy. This radiation illuminates the CH sphere through a 0.2×2 mm^2 diamond window mounted over a diagnostic hole on the hohlraum wall. Another diamond window on the opposite side of the hohlraum allows for streaked radiography, giving time-resolved measurements of density, opacity, and pressure of the imploding sphere [12]. The scattered radiation is simultaneously collected by a high-efficiency, mono-angle crystal spectrometer [17,18] using a cylindrically curved, highly oriented pyrolytic graphite (HOPG) crystal that has a line of sight towards the imploded plastic sphere through the upper laser entrance hole. A 50-μm-thick gold foil added to the hohlraum blocks the direct path of the probe radiation towards the spectrometer. Due to the size of the plasma source, partly blowing beyond the shielding, the spectral region usable for data analysis is limited to 8600–9200 eV. A gated x-ray detector (GXD) allows for time-resolved snapshots of the scattered radiation to be taken with 100 ps integration time. The GXD timing was chosen to be 480 ps after shock coalescence in the center of the imploding sphere.

Although the CH sample exhibits distinct radial gradients at the time of probing (see Fig. 2), a previous numerical study [19] finds that the scattered radiation intensity is strongly dominated by certain parts of the CH target. For a low-adiabat drive with four shocks, one mainly tests the relatively cold, low-density material around the ablation front [19]. Here, we apply a simpler two-shock drive [13] increasing the sensitivity to the bulk of compressed inward moving material surrounding the hot dense core. Thus, we expect scattering from hot, dense matter at moderately coupled conditions to dominate the measured signal.

The measurements described here were obtained by XRTS of $\sim$9 keV monoenergetic x rays at a scattering angle of 84° in the noncollective scattering regime [11]. This method is a unique tool to assess the basic properties of the plasma as the scattering spectrum is directly related to the velocity distribution of the free electrons [20–22], the plasma composition, and spatial correlations between the ions [23–28]. Here, we demonstrate the high sensitivity of XRTS to probe inner-shell ionization in highly compressed matter with high accuracy in the extreme environments of implosions driven by the NIF laser.

The x-ray photons from the Zn He-α probe are scattered from the electrons in the compressed plastic sample. For locally isotropic conditions, the double-differential cross section of this process is given by [29,30]

$$\frac{\partial^2 \sigma}{\partial \omega \, \partial \Omega} = \sigma_T \frac{\omega_s}{\omega_i} \frac{1}{2} \left(1 + \cos^2 \theta\right) S(k,\omega), \qquad (1)$$

where σ_T is the Thomson scattering cross section, ω_i the frequency of the incident radiation, ω_s the frequency of the scattered radiation, $\omega = \omega_i - \omega_s$ the frequency shift, and $k = |\mathbf{k_i} - \mathbf{k_s}| = 2\omega_i \sin(\theta/2)/c$ is the scattering wave number for a given scattering angle θ. $S(k,\omega)$ denotes the total dynamic electron structure factor, which contains all spatial and temporal information on the microscopic correlations

between the electrons in the sample. Considering the ions in a static approximation, the total electron structure factor can be decomposed into two terms [31]

$$S(k,\omega) = W_{el}(k)\delta(\omega) + W_{inel}(k,\omega), \quad (2)$$

where $W_{el}(k)$ accounts for elastic scattering from bound electrons and electrons forming the screening cloud, both dynamically following the ion motion, and $W_{inel}(k,\omega)$ is the spectral strength of inelastic scattering from free and weakly bound electrons.

For multicomponent systems such as CH, the elastic scattering strength contains single-species contributions of each component as well as cross-correlations between different ion species. All contributions for the elastic scattering strength can be summarized as [32]

$$W_{el}(k) = \sum_{a,b} \sqrt{x_a x_b}[f_a(k) + q_a(k)][f_b(k) + q_b(k)]S_{ab}(k), \quad (3)$$

where $x_{a,b}$ are the number fractions of the different ion components, $f_{a,b}(k)$ denote the atomic form factors, $q_{a,b}(k)$ the Fourier density of the screening cloud, and $S_{ab}(k)$ are the partial ion structure factors. For large k (here, $k = 6.1 \, \text{Å}^{-1}$), the elastic scattering is dominated by tightly bound inner-shell electrons, thus determining the ratio of elastic and inelastic scattering results in strong sensitivity for carbon K-shell ionization in our experiments.

The inelastic scattering part for the multicomponent system is the sum of single species contributions and can be written as

$$W_{inel}(k,\omega) = S_{ee}^0(k,\omega) \sum_a x_a Z_a^f + \sum_a x_a S_a^{be}(k,\omega), \quad (4)$$

where Z_a^f are the average charge states of the different ion species, and $S_{ee}^0(k,\omega)$ and $S_a^{be}(k,\omega)$ denote the structure factors of the free electrons in the plasma and inelastic bound-free scattering events, respectively.

In order to more comprehensively analyze the data acquired in this experiment, the strong plasma gradients present in the sample should be considered. As a first simple approximation, we fit the data by varying a global temperature T and carbon charge state Z_C when calculating synthetic spectra [zero dimensional (0D) approach]; the density is kept fixed as it has been independently measured by radiography. These results will be compared with the mass-weighted averages $\langle T \rangle$ and $\langle Z_C \rangle$ of predictions from the HYDRA simulations. Here, we define the averages as

$$\langle X \rangle = \frac{\int_0^\infty r^2 \rho(r) X(r) dr}{\int_0^\infty r^2 \rho(r) dr}, \quad (5)$$

where $X(r)$ denotes the radial profile of quantity X.

The one-dimensional HYDRA simulations predict at the time of probing $\langle \rho \rangle = 6.74 \, \text{g cm}^{-3}$, $\langle T \rangle = 109$ eV, and $\langle Z_C \rangle = 4.40$, corresponding to a pressure of ~ 35 TPa. The prediction for the radial density profile is in good agreement with time-resolved radiography measurements, which were performed in the same experiment. Thus, we only vary T and Z_C in order to match the measured XRTS spectrum. This 0D fit yields $\langle T \rangle = 86 \pm 20$ eV and $\langle Z_C \rangle = 4.92 \pm 0.15$ (see Fig. 3),
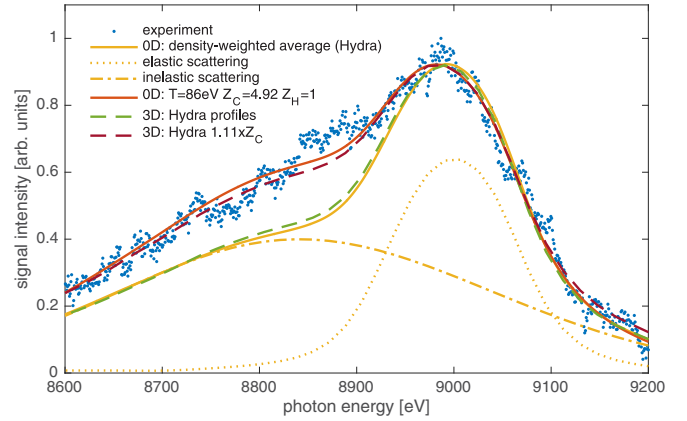

FIG. 3. Comparison of experimental data with synthetic scattering spectra using the full 3D ray-tracing and weighting scheme.

therefore predicting significantly higher carbon ionization than suggested by simulations, while simultaneously giving reasonable agreement for the temperature of the bulk plasma. For the elastic scattering strength we extract $W_{el} = 0.85$ and a ratio of elastic to total scattering of $W_{el}/S = 0.24$. Using the ionization from the simulations would result in $W_{el} = 1.39$ and $W_{el}/S = 0.35$, which underlines the strong sensitivity of the elastic scattering to carbon K-shell ionization. The quoted error bars for $\langle Z_C \rangle$ and $\langle T \rangle$ are largely dominated by accounting for possible systematic errors in the background subtraction [33]. The theoretical model for the fit employs a multicomponent hypernetted chain model for the static ion structure [34], finite-wavelength screening [35], and the Born-Mermin approximation with local field corrections for the free-free component of the inelastic feature [36]. Using the simpler screened one-component model [37] for the elastic feature, we obtain a similar temperature, but the ion charge state obtained is even higher: $\langle Z_C \rangle = 5.11 \pm 0.2$.

For a more detailed understanding, spatial gradients, the attenuation of probe radiation inside the sample, and spectral blurring due to the extended sample size have to be included in the analysis of the scattering spectrum. Contributions of different sample regions are calculated by a previously developed weighting scheme that considers density as well as opacity effects [19]. In order to assess the extended sample size, a ray-tracing scheme has been implemented following rays from the source plasma through the sample to the HOPG crystal and the detector. Besides spectral blurring, this method also accounts for the range of scattering angles present due to the large sample size. Further details on the three-dimensional (3D) weighting scheme can be found in the Supplemental Material [33].

Figure 3 shows a comparison between the XRTS spectrum obtained 480 ps after shock coalescence at $r = 0$ and theoretical predictions using 0D and full 3D calculations of the spectrum based on the HYDRA simulations. These predictions contain an instrument function that implements a spectral blur due to the extended sample size and the effective scattering angle. Moreover, the models are normalized to the strength of the measured elastic scattering feature.

When comparing the simple 0D application of density-weighted average temperature and ionization degree to the
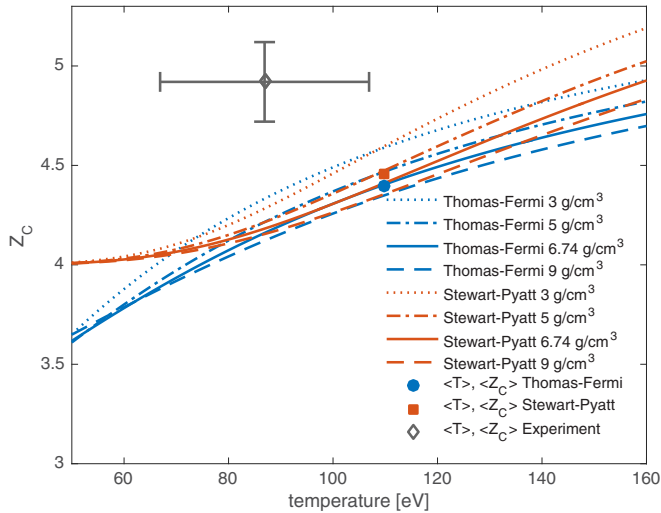
FIG. 4. Comparison of the 0D fit results with Thomas-Fermi and Stewart-Pyatt predictions for the carbon ionization when varying density and temperature.
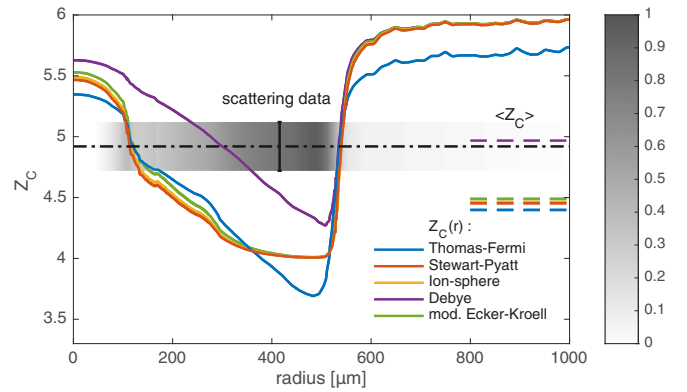

FIG. 5. Ionization degree of the carbon component predicted by various models for radial density and temperature profiles calculated by HYDRA simulations at the time of probing. The short lines on the right are the predictions for the average conditions in the sample. The gray shaded area gives the best fit to the experiment with error bars in the vertical direction. The gray scale in the horizontal direction indicates the weight $r^2\rho(r)$ of this radial region.

results from the full 3D calculations, it is apparent that the difference is rather small despite the substantial gradients inside the sample. This result is due to the heavy weighting of the signal from the large volume of relatively homogeneous bulk plasma outside of the highly compressed core. Thus, the shape of both the measured and synthetic spectra reflect the conditions of this region. Figure 3 further demonstrates that the Thomas-Fermi-type equation of state is not adequate to model the conditions probed. A much better match to the data is obtained when artificially increasing the carbon ionization by 11%.

A comparison between the 0D fit results and standard models for the carbon ionization at different densities and temperatures is shown in Fig. 4. Obviously, the Thomas-Fermi approach applied in the hydrodynamic simulations cannot reproduce the measurements, even when significantly varying density and temperature. To improve the description of the ionization balance, we have solved a system of Saha equations for the CH plasma [33] that considers the discrete ionization levels of the ions and applies the Stewart-Pyatt model for the ionization potential depression. In the regime of the density weighted averages predicted by the hydrodynamic simulations, there is excellent agreement with Thomas-Fermi, and thus, the experimental results cannot be matched as well.

Assessing the effects of gradients inside the sample, Fig. 5 illustrates predictions for radial ionization profiles for Thomas-Fermi and the Saha scheme. This shows that proper averaging only slightly increases $\langle Z_C \rangle$ above the 0D model predictions in Fig. 4. Besides Thomas-Fermi and Stewart-Pyatt, we also tested other common analytical models: ion sphere, Debye, and a modified Ecker-Kroell model [9,33]. For radii between 200 and 600 μm, which dominate our scattering results, most approaches give similar results. Only the average charge state predicted by the Debye scheme, assuming linear screening and including quantum corrections, results in increased carbon ionization in reasonable agreement with the experiment. This close match is certainly surprising and may be accidental since, despite relatively weak coupling

of the electrons [$\Gamma_{ee} \sim 0.1$ with $\Gamma_{aa} = Z_a^2 e^2/(k_B T r_a)$ where r_a is the mean distance between two particles of species a], the carbon ions are significantly coupled ($\Gamma_{CC} \gtrsim 1$). With that, the Debye picture is certainly at or beyond the edge of its physical justification and therefore, more sophisticated models and further experiments will be required for a better understanding. Nevertheless, the widely applied Stewart and Pyatt model yields very poor results similar to the ion-sphere model, both underpredicting $\langle Z_C \rangle$. This result holds as well when considering the numerically calculated correction factor given in Stewart and Pyatt's original publication [7]. This factor increases the values for the ionization potential depression by 15%–20%, giving values similar to the modified Ecker-Kroell model in our case. Thus, our experimental data suggest that the ion sphere limit is inadequate in this previously untested regime of high densities and temperatures. So far, there is no reliable and practical *ab initio* technique to obtain predictions for the regime that has been probed in our experiment.

In conclusion, we have presented results from a spectrally resolved x-ray scattering measurement at the National Ignition Facility determining the (mass-weighted) average temperature and ionization of an imploded plastic sphere. In particular, the degree of K-shell ionization is inferred with high sensitivity from the strength of elastic x-ray scattering. The carbon charge states consistent with the scattering data are substantially higher than predicted by HYDRA when applying a Thomas-Fermi-type equation of state. Our results also suggest that the widely used Stewart-Pyatt formula, and with that the ion sphere limit for the ionization potential depression, is not applicable for the extreme conditions probed by our experiment. This result has important implications for the modeling of ICF ablators as well as many astrophysical objects having similar extreme conditions [1] as the macroscopic properties of such systems crucially depend on the ionization balance. More precise ionization measurements applying a newly developed x-ray scattering platform at the National Ignition Facility are on the way [38].

[1] V. E. Fortov, *Extreme States of Matter on Earth and in the Cosmos* (Springer, New York, 2011).

[2] O. A. Hurricane *et al.*, Nature (London) **506**, 343 (2014).

[3] T. Döppner *et al.*, Phys. Rev. Lett. **115**, 055001 (2015).

[4] J. C. Pain, Contrib. Plasma Phys. **47**, 421 (2007).

[5] L. B. Fletcher, A. L. Kritcher, A. Pak, T. Ma, T. Döppner, C. Fortmann, L. Divol, O. S. Jones, O. L. Landen, H. A. Scott, J. Vorberger, D. A. Chapman, D. O. Gericke, B. A. Mattern, G. T. Seidler, G. Gregori, R. W. Falcone, and S. H. Glenzer, Phys. Rev. Lett. **112**, 145004 (2014).

[6] U. Zastrau, P. Sperling, M. Harmand, A. Becker, T. Bornath, R. Bredow, S. Dziarzhytski, T. Fennel, L. B. Fletcher, E. Forster, S. Göde, G. Gregori, V. Hilbert, D. Hochhaus, B. Holst, T. Laarmann, H. J. Lee, T. Ma, J. P. Mithen, R. Mitzner, C. D. Murphy, M. Nakatsutsumi, P. Neumayer, A. Przystawik, S. Roling, M. Schulz, B. Siemer, S. Skruszewicz, J. Tiggesbaumker, S. Toleikis, T. Tschentscher, T. White, M. Wostmann, H. Zacharias, T. Döppner, S. H. Glenzer, and R. Redmer, Phys. Rev. Lett. **112**, 105002 (2014).

[7] J. C. Stewart and K. D. Pyatt, Astrophys. J. **144**, 1203 (1966).

[8] S. M. Vinko *et al.*, Nature (London) **482**, 59 (2012).

[9] O. Ciricosta, S. M. Vinko, H. K. Chung, B. I. Cho, C. R. D. Brown, T. Burian, J. Chalupsky, K. Engelhorn, R. W. Falcone, C. Graves, V. Hajkova, A. Higginbotham, L. Juha, J. Krzywinski, H. J. Lee, M. Messerschmidt, C. D. Murphy, Y. Ping, D. S. Rackstraw, A. Scherz, W. Schlotter, S. Toleikis, J. J. Turner, L. Vysin, T. Wang, B. Wu, U. Zastrau, D. Zhu, R. W. Lee, P. Heimann, B. Nagler, and J. S. Wark, Phys. Rev. Lett. **109**, 065002 (2012).

[10] D. J. Hoarty, P. Allan, S. F. James, C. R. D. Brown, L. M. R. Hobbs, M. P. Hill, J. W. O. Harris, J. Morton, M. G. Brookes, R. Shepherd, J. Dunn, H. Chen, E. Von Marley, P. Beiersdorfer, H. K. Chung, R. W. Lee, G. Brown, and J. Emig, Phys. Rev. Lett. **110**, 265003 (2013).

[11] S. H. Glenzer and R. Redmer, Rev. Mod. Phys. **81**, 1625 (2009).

[12] A. L. Kritcher *et al.*, High Energy Density Phys. **10**, 27 (2014).

[13] S. Le Pape, L. Divol, L. Berzak Hopkins, A. Mackinnon, N. B. Meezan, D. Casey, J. Frenje, H. Herrmann, J. McNaney, T. Ma, K. Widmann, A. Pak, G. Grimm, J. Knauer, R. Petrasso, A. Zylstra, H. Rinderknecht, M. Rosenberg, M. Gatu-Johnson, and J. D. Kilkenny, Phys. Rev. Lett. **112**, 225002 (2014).

[14] M. M. Marinak, S. W. Haan, T. R. Dittrich, R. E. Tipton, and G. B. Zimmerman, Phys. Plasmas **5**, 1125 (1998).

[15] B. Bachmann *et al.*, Rev. Sci. Instrum. **85**, 11D614 (2014).

[16] D. Kraus *et al.*, Rev. Sci. Instrum. **85**, 11D606 (2014).

[17] T. Döppner *et al.*, J. Phys.: Conf. Ser. **500**, 192019 (2014).

[18] T. Döppner *et al.*, Rev. Sci. Instrum. **85**, 11D617 (2014).

[19] D. A. Chapman *et al.*, Phys. Plasmas **21**, 082709 (2014).

[20] S. H. Glenzer, G. Gregori, R. W. Lee, F. J. Rogers, S. W. Pollaine, and O. L. Landen, Phys. Rev. Lett. **90**, 175002 (2003).

[21] H. J. Lee, P. Neumayer, J. Castor, T. Doppner, R. W. Falcone, C. Fortmann, B. A. Hammel, A. L. Kritcher, O. L. Landen, R. W. Lee, D. D. Meyerhofer, D. H. Munro, R. Redmer, S. P. Regan, S. Weber, and S. H. Glenzer, Phys. Rev. Lett. **102**, 115001 (2009).

[22] A. L. Kritcher, T. Döppner, C. Fortmann, T. Ma, O. L. Landen, R. Wallace, and S. H. Glenzer, Phys. Rev. Lett. **107**, 015002 (2011).

[23] E. Garcia Saiz *et al.*, Nat. Phys. **4**, 940 (2008).

[24] T. Ma, T. Döppner, R. W. Falcone, L. Fletcher, C. Fortmann, D. O. Gericke, O. L. Landen, H. J. Lee, A. Pak, J. Vorberger, K. Wunsch, and S. H. Glenzer, Phys. Rev. Lett. **110**, 065001 (2013).

[25] D. Kraus, J. Vorberger, D. O. Gericke, V. Bagnoud, A. Blazevic, W. Cayzac, A. Frank, G. Gregori, A. Ortner, A. Otten, F. Roth, G. Schaumann, D. Schumacher, K. Siegenthaler, F. Wagner, K. Wunsch, and M. Roth, Phys. Rev. Lett. **111**, 255501 (2013).

[26] S. White *et al.*, High Energy Density Phys. **9**, 573 (2013).

[27] L. B. Fletcher *et al.*, Nat. Photonics **9**, 274 (2015).

[28] D. Kraus *et al.*, Phys. Plasmas **22**, 056307 (2015).

[29] J. Sheffield, D. Froula, S. H. Glenzer, and J. N. C. Luhmann, *Plasma Scattering of Electromagnetic Radiation* (Academic, New York, 2011).

[30] B. J. B. Crowley and G. Gregori, New J. Phys. **15**, 015014 (2013).

[31] J. Chihara, J. Phys.: Condens. Matter **12**, 231 (2000).

[32] K. Wünsch, J. Vorberger, G. Gregori, and D. O. Gericke, Europhys. Lett. **94**, 25001 (2011).

[33] See Supplemental Material at http://link.aps.org/supplemental/10.1103/PhysRevE.94.011202 for a detailed description of uncertainties due to background subtraction and spatial gradients inside the sample, and a discussion of the applied ionization models which are used to interpret the acquired data.

[34] K. Wünsch, P. Hilse, M. Schlanges, and D. O. Gericke, Phys. Rev. E **77**, 056404 (2008).

[35] D. A. Chapman *et al.*, Nat. Commun. **6**, 6839 (2015).

[36] R. Thiele, T. Bornath, C. Fortmann, A. Höll, R. Redmer, H. Reinholz, G. Röpke, A. Wierling, S. H. Glenzer, and G. Gregori, Phys. Rev. E **78**, 026411 (2008).

[37] G. Gregori, A. Ravasio, A. Höll, S. H. Glenzer, and S. J. Rose, High Energy Density Phys. **3**, 99 (2007).

[38] D. Kraus *et al.*, J. Phys.: Conf. Ser. **717**, 012067 (2016).